frontiers | Frontiers in Materials

TYPE Original Research
PUBLISHED 30 May 2024
DOI 10.3389/fmats.2024.1407655

OPEN ACCESS

EDITED BY
Wenwen Dou,
Shandong University, China

REVIEWED BY
Weichen Xu,
Chinese Academy of Sciences (CAS), China
Enze Zhou,
Northeastern University, China

*CORRESPONDENCE
Tingyue Gu,
gu@ohio.edu

RECEIVED 27 March 2024
ACCEPTED 10 May 2024
PUBLISHED 30 May 2024

CITATION
Xu L, Khan A, Kijkla P, Kumseranee S, Punpruk S and Gu T (2024), Prevention of severe pitting corrosion of 13Cr pipeline steel by a sulfate reducing bacterium using a green biocide cocktail.
Front. Mater. 11:1407655.
doi: 10.3389/fmats.2024.1407655

Prevention of severe pitting corrosion of 13Cr pipeline steel by a sulfate reducing bacterium using a green biocide cocktail

Lingjun Xu[1], Adnan Khan[2], Pruch Kijkla[3], Sith Kumseranee[3], Suchada Punpruk[3] and Tingyue Gu[1,2]*

[1]Department of Chemical and Biomolecular Engineering, Institute for Corrosion and Multiphase Technology, Ohio University, Athens, OH, United States, [2]Department of Biological Sciences, Molecular and Cellular Biology Program, Ohio University, Athens, OH, United States, [3]PTT Exploration and Production, Bangkok, Thailand

To combat abiotic CO_2 corrosion of pipelines, chromium steels (CrSs) are used to replace carbon steels, but CrSs can suffer very severe pitting corrosion caused by microbiologically influenced corrosion (MIC) because their passive films are not as good as those on high-grade stainless steels, and their MIC often involves (semi-)conductive corrosion product films. In this study, severe pitting corrosion (2.0 cm/a pitting corrosion rate) with a 7-day weight loss of 3.8 ± 0.5 mg/cm^2 (0.26 mm/a uniform corrosion rate) was observed on 13Cr coupons incubated anaerobically with a highly corrosive pure-strain sulfate reducing bacterium (SRB) *Desulfovibrio ferrophilus* IS5 in 125 mL anaerobic vials filled with 50 mL enriched artificial seawater at 28°C. A popular green biocide, namely tetrakis hydroxymethyl phosphonium sulfate (THPS), was enhanced by biofilm dispersing Peptide A (a 14-mer) to mitigate SRB MIC against 13Cr. The 7-day weight losses for coupons with 50 ppm (w/w) THPS, 50 ppm THPS + 100 nM (180 ppb) Peptide A and 100 ppm THPS were reduced to 2.2 ± 0.2 mg/cm^2, 1.5 ± 0.5 mg/cm^2, and 0.3 ± 0.2 mg/cm^2, respectively. The pitting rates also decreased from 20 mm/a to 12 mm/a, 8.6 mm/a, and 1.5 mm/a, respectively based on the maximum pit depth data for the 7-day incubation. Electrochemical tests using a miniature electrochemical glass cell design supported the weight loss trend with additional transient corrosion rate information. THPS was found to be effective in mitigating severe pitting corrosion on 13Cr, and the enhancement effect of Peptide A for THPS was manifested. This work has significant implications in field applications when CrSs are considered as metal choices to replace carbon steels to combat abiotic CO_2 corrosion in pipelines. When SRB MIC is a possible threat, a mitigation plan needs to be implemented to prevent potentially very severe pitting that can lead to pinhole leaks.

KEYWORDS

microbiologically influenced corrosion, sulfate reducing bacterium, 13Cr, pitting corrosion, biocide mitigation

1 Introduction

It is known that microbiologically influenced corrosion (MIC) is a serious menace to various assets in the oil and gas industry (D. Xu et al., 2023; Yazdi et al., 2021). It has been reported to be responsible for nearly 20% of the total corrosion costs (Kermani and Harrop, 1996; Skovhus et al., 2017). Different types of microorganisms including bacteria, archaea, fungi, and microalgae have been documented to cause deterioration of various metals directly and indirectly (Chugh et al., 2020; El-Shamy, 2020; You et al., 2021). Sulfate reducing bacteria (SRB) have been extensively studied in MIC research since they are ubiquitous in the environment, especially anaerobic environment, and very aggressive to metals (Videla and Characklis, 1992; Sand and Gehrke, 2003; Abdullah et al., 2014; Enning and Garrelfs, 2014; Yang et al., 2020). They typically utilize sulfate as the terminal electron acceptors through the respiration process to obtain energy from organic compounds or H_2 (Černoušek et al., 2020). The corrosion mechanisms of SRB are mainly categorized into extracellular electron transfer-MIC (EET-MIC) and metabolite-MIC (M-MIC) (Wang et al., 2020; Pu et al., 2023).

EET-MIC occurs when a metal such as Fe^0 is energetic enough to serve as the electron donor for sulfate reduction. During this process, electrons released from iron oxidation Eq. 1 are transported across cell walls and finally used for enzyme-catalyzed sulfate reduction Eq. 2 to in the SRB cytoplasm (Gu et al., 2019).

$$\text{Oxidation}: 4Fe \rightarrow 4Fe^{2+} + 8e^- \left(E^\circ = -447\,mV_{SHE}\right) \quad (1)$$

$$\text{Reduction}: SO_4^{2-} + 9H^+ + 8e^- \rightarrow HS^- + 4H_2O \left(E^{\circ\prime} = -217\,mV_{SHE}\right) \quad (2)$$

The apostrophe in $E^{\circ\prime}$ indicates pH 7 physiological condition in bioenergetics (Thauer et al., 2007). Another major type of MIC happens to metals (e.g., Cu) that are not energetic enough to donate electrons to facilitate sulfate reduction. In this case, M-MIC is the mechanism for SRB MIC of Cu.

$$2Cu + HS^- + H^+ \rightarrow Cu_2S + H_{2(g)} \left(\Delta G^{\circ\prime} = -58.3\,kJ/mol\right) \quad (3)$$

Due to the extremely low solubility of Cu_2S, the reaction in Eq. 3 has a rather negative Gibbs free energy change. This corrosion reaction is thermodynamically favorable and H^+ becomes a feasible electron acceptor in M-MIC (Blais et al., 2008; Gu et al., 2019).

Active metals such as Al and Zn can be easily corroded by water hydrolysis when their oxide passive films are damaged. These mineral films can be damaged by biofilms which lead to FD-MIC (film-damage MIC) (Unsal et al., 2021).

SRB MIC of metals containing Fe^0 is known to be EET-MIC because it can be accelerated by an electron mediator such as riboflavin and conductive magnetite nanoparticles (MNPs) (Wang et al., 2022b). Furthermore, starved sessile cells were found to be far more corrosive (Xu and Gu, 2014). In EET-MIC, more sessile cells harvest more electrons to harvest energy in their respiration (Jia et al., 2018). Thus, mitigation of EET-MIC needs to reduce the sessile cell count.

Different materials such as carbon steels (CSs), chromium steels (CrSs) and stainless steels (SSs) are used in the oil and gas industry (Hinds et al., 2005; Mesquita et al., 2014; Obot et al., 2020; Costa et al., 2023). Their corrosion behaviors under different conditions have been widely studied (Dorcheh et al., 2016; Alcántara et al., 2017; Dwivedi et al., 2017; Fahim et al., 2019; Dong et al., 2020; Ettefagh et al., 2021). Compared with CSs, SSs provide higher corrosion resistance to CO_2 due to the Cr-rich passive film on the surface (Wu et al., 2013; Lin et al., 2015; Wang et al., 2016). CrSs are the economical alternative to expensive SSs in combating abiotic CO_2 corrosion, which usually appears as uniform corrosion. However, in SRB MIC, CrSs or low grade SSs were found to suffer severe pitting corrosion despite their high uniform corrosion resistance (Xu et al., 2023b). Unlike the non-conductive siderite film in CO_2 corrosion, the semi-conductive FeS film in SRB MIC allows electrons to be harvested across it. The occasionally damaged spots on the Cr-rich layer will serve as anodic sites where iron oxidation will occur. The much larger undamaged surface becomes a large cathode, and the small anode-large cathode area ratio situation amplifies pitting. In a previous study, 13Cr [also known as API 5CT L80-13Cr, 13Cr or 420 SS (Scheuer et al., 2019)] incubated with *Desulfovibrio ferrophilus* (IS5 strain) for 7 days had a much lower weight loss of 4.4 mg/cm^2 (0.30 mm/a uniform corrosion rate) compared with N80 carbon steel (15.2 mg/cm^2 and 1.01 mm/a uniform corrosion rate). However, 13Cr suffered very severe pitting corrosion (15 mm/a) compared with N80 (0.38 mm/a), with 7-day pits visible even to the naked eyes (L. Xu et al., 2023b).

The relative pitting severity (*RPS*) was defined by Eq. 4 to quantify the pitting corrosion severity vs. uniform corrosion severity (Dou et al., 2018),

$$RPS = \frac{\text{maximum pitting rate}}{\text{uniform corrosion rate based on (specific) weight loss}} \quad (4)$$

When *RPS* is around unity, both pitting corrosion and uniform corrosion are important. When *RPS* is much greater than unity, pitting corrosion is deemed much more aggressive than uniform corrosion. The *RPS* of 13Cr in *D. ferrophilus* IS5 MIC was found to be 50 in SRB MIC which is far greater than unity, indicating very high pitting corrosion relatively to uniform corrosion (L. Xu et al., 2023b). Pitting corrosion is more dangerous than uniform corrosion since deep pits can easily lead to pipeline failures due to pinhole leaks (Chouchaoui and Pick, 1996; Abdalla Filho et al., 2014). Even a single deep pit can penetrate the material and cause equipment failure and even catastrophic accidents (Bhandari et al., 2015). Therefore, a mitigation plan should be in place to minimize pitting risks of 13Cr.

Biocide mitigation is a common strategy to treat biofilms which are responsible for MIC (Grande Burgos et al., 2013; Astuti et al., 2018; Abbas et al., 2021). Tetrakis hydroxymethyl phosphonium sulfate (THPS) is a popular green biocide in oilfields which has been found to be effective in mitigating SRB MIC in different systems (Gana et al., 2011; Conlette, 2014; Silva et al., 2021). Biocide enhancers at a small dosage can considerably improve biocide efficacy when used together with biocides (Mukherjee and Ahn, 2022; Xu et al., 2023a; Shi et al., 2023). Peptide A, a chemically synthesized 14-mer circular peptide (cys-ser-val-pro-tyr-asp-tyr-asn-trp-tyr-ser-asn-trp-cys) was reported to be an effective biocide enhancer at a sub-ppm (w/w) dosage for THPS in mitigating MIC. It is a nature-mimicking peptide that shows a biofilm dispersing effect in the presence of biocides. Its core 12-mer sequence was inspired

TABLE 1 Test matrix to evaluate biocide mitigation of *D. ferrophilus* MIC against 13Cr.

Parameter	Condition
Microbe	*D. ferrophilus* (IS5 strain)
Cultural medium	Enriched artificial seawater (EASW)
Coupon material	13Cr
Liquid volume	50 mL in 125 mL anaerobic vials, 5 mL in 10 mL glass cells
Inoculum size	0.5 mL in anaerobic vials, 0.05 mL in glass cells
Temperature	28°C
Initial pH	7.0 ± 0.2
Incubation time	7 days
Treatment	No treatment (control), 50 ppm THPS, 50 ppm THPS + 100 nM (180 ppb) Peptide A, 100 ppm THPS
Assay	Sessile cell count, weight loss, pit depth using 125 mL anaerobic vials; electrochemical tests using 10 mL glass cells

by nature with its origin from a protein in a sea anemone that has a biofilm-free exterior (Jia et al., 2019). A biocide such as THPS at a low concentration may achieve the same inhibition result as a high concentration with the help of Peptide A at a sub-ppm dosage.

Because of the potential severe pitting on 13Cr caused by SRB MIC, for field applications it is necessary to have mitigation strategies such as biocide treatment in place. Thus, it is desired to study if deep pits would disappear with biocide treatment. In this work, 13Cr coupons were incubated with *D. ferrophilus* IS5, a highly corrosive SRB strain. Different biocide dosages were tested to investigate the mitigation effect of THPS and enhancement performance of Peptide A. The coupon tests were complimented by electrochemical tests.

2 Experimental

2.1 Bacterium, metal, and culture medium

Table 1 shows a test matrix for this investigation. *D. ferrophilus* (strain IS5) was cultured anaerobically in enriched artificial seawater (EASW) culture medium at 28°C (optimal temperature for growth) (Enning et al., 2012). The composition of EASW is listed in Table 2. The test coupon was 13Cr, and its elemental composition is summarized in Table 3.

The EASW culture medium was adjusted to an initial pH of 7.0 using 5% (w/w) NaOH. Before inoculation, the medium was autoclave-sterilized and deoxygenated by purging filter-sterilized N_2 gas for 1 h. The addition of 100 ppm (w/w) L-cysteine into EASW was conducted in an anaerobic chamber filled with N_2 to further remove dissolved oxygen, following its use in the ATCC 1249 culture medium. THPS (Sigma-Aldrich, St. Louis, MO, USA) was dissolved into a 5,000 ppm (w/w) stock solution for biocide treatment.

TABLE 2 Composition of EASW culture medium (Sheng et al., 2007).

Chemical	Amount
NaCl	23.476 g
Na_2SO_4	3.917 g
$NaHCO_3$	0.192 g
KCl	0.664 g
KBr	0.096 g
H_3BO_3	0.026 g
$MgCl_2$	4.965 g
$SrCl_2{\cdot}6H_2O$	0.04 g
$CaCl_2{\cdot}2H_2O$	1.469 g
Sodium lactate	3.5 g
Yeast extract	1.0 g
Sodium citrate	0.5 g
$MgSO_4{\cdot}7H_2O$	0.71 g
$CaSO_4{\cdot}2H_2O$	0.1 g
NH_4Cl	0.1 g
K_2HPO_4	0.05 g
$Fe(NH_4)_2(SO_4)_2{\cdot}6H_2O$	1.37 g
DI water	1 L

The pre-cut 13Cr coupons all had an exposed top surface area of 1 cm^2 (1 cm × 1 cm). The top test surfaces were polished progressively to a 600 grit final finish. All other coupon surfaces were painted with inert Epoxy coating (3M Product 323). The coupons were sanitized using absolute isopropanol before testing.

2.2 Enumeration of sessile cells

Three replicate 13Cr coupons were put into each anaerobic vial for different treatment conditions. The initial *D. ferrophilus* planktonic cell concentration in each vial upon inoculation was 10^6 cells/mL. After incubation for 7 days, all coupons were taken out from the anaerobic vials. Deoxygenated phosphate buffered saline (PBS) solution (pH 7.4) was then used to rinse the coupons. Sessile cells on each coupon surface were transferred into a 10 mL (or 1 mL if cell count too low for counting in a 10 mL cell suspension) PBS solution (total) using a sterile brush applicator. The brush, the coupon, and the PBS solution were vortexed for 30 s in a 50 mL centrifuge tube. The evenly distributed cell suspension in the tube was used for cell counting. A hemocytometer was employed in which (viable motile) cells can be counted under an optical microscope at ×400 magnification.

10.3389/fmats.2024.1407655

TABLE 3 Elemental compositions (wt%) of 13Cr (Fe balance).

C	Mn	Cr	Ni	Cu	P	S	Si
0.15–0.22	0.25–1.00	12.0–14.0	≤0.50	≤0.25	≤0.020	≤0.010	≤1.00

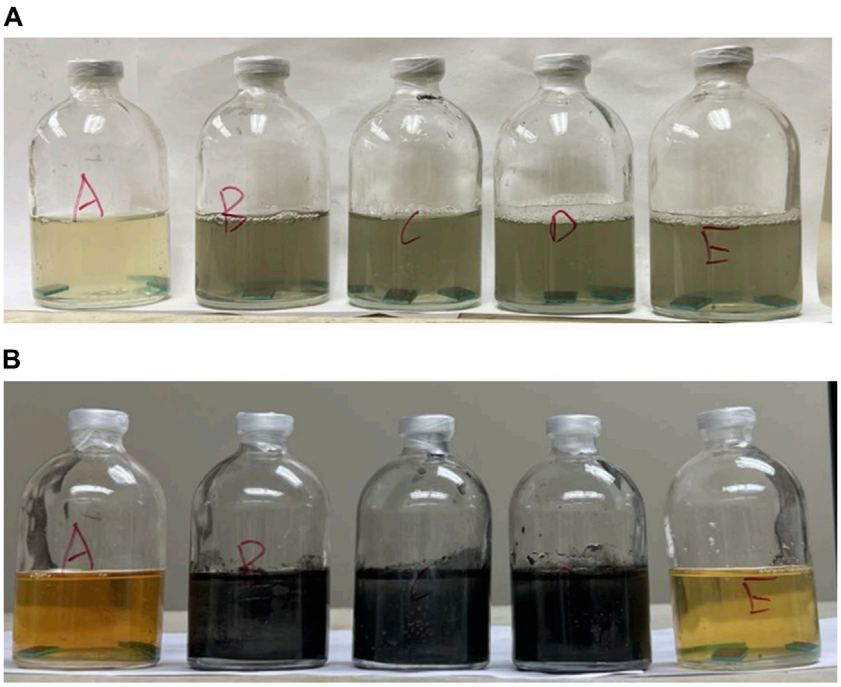

FIGURE 1
Anaerobic vials containing 13Cr coupons before **(A)** and after **(B)** 7-day incubation with *D. ferrophilus* (strain IS5) in EASW (left to right): abiotic control, no treatment, 50 ppm THPS, 50 ppm THPS + 100 nM Peptide A, and 100 ppm THPS.

TABLE 4 Sessile cell count and reduction in biofilms on 13Cr coupon surfaces.

Treatment	Sessile cell count ($\times 10^6$ cells/cm^2)	Reduction
No treatment	39 ± 8	-
50 ppm THPS	8.0 ± 0.4	0.7-log
50 ppm THPS + 100 nM Peptide A	2.4 ± 0.4	1.2-log
100 ppm THPS	Undetectable	(>2.9-log)

2.3 Biofilm visualization

Biofilms on coupon surfaces after 7-day incubation were observed under CLSM (confocal laser scanning microscopy) (Model LSM 510, Carl Zeiss, Jena, Germany). Coupons were first rinsed in pH 7.4 PBS solution to wash away planktonic cells and culture medium. Then the coupon surfaces were stained with Live/Dead® BacLight™ Bacterial Viability Kit L7012 (Life Technologies, Grand Island, NY, United States) before observation. Under CLSM, live cells were seen as green dots at 488 nm wavelength laser and dead cells as red dots at a wavelength of 559 nm.

2.4 Weight loss and pit depth

Three replicate 13Cr coupons were used for each treatment condition in the weight loss test. After the 7-day incubation in 125 mL anaerobic vials, the biofilm and corrosion products on each coupon were removed with a freshly prepared Clarke's solution for 30 s before weight measurement following ASTM G1–03. Coupon surfaces were scanned using an infinite focus microscope (IFM) profilometer (Model ALC13, Alicona Imaging GmbH, Graz, Austria) to obtain pit depth and surface profiles.

2.5 Electrochemical measurements

Electrochemical tests were executed in 10 mL electrochemical glass cells, each filled with 5 mL EASW inoculated with 0.05 mL

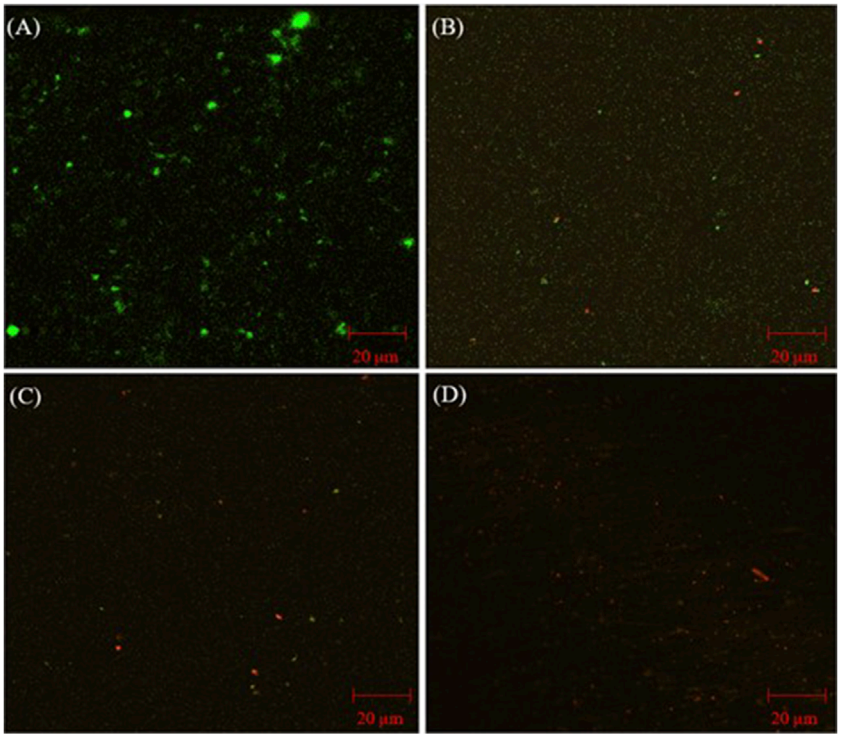

FIGURE 2
CLSM images of biofilms on 13Cr coupons after 7-day incubation *D. ferrophilus* in EASW: **(A)** no treatment, **(B)** 50 ppm THPS, **(C)** 50 ppm THPS + 100 nM Peptide A, and **(D)** 100 ppm THPS.

TABLE 5 Weight loss of 13Cr after 7-day incubation with *D. ferrophilus*.

Treatment	Weight loss (mg/cm^2)	Uniform corrosion rate (mm/a)	Inhibition efficiency (%)
Abiotic	−0.1 ± 0.1	−0.01 ± 0.01	-
No treatment	3.8 ± 0.5	0.26 ± 0.03	(basis)
50 ppm THPS	2.2 ± 0.2	0.15 ± 0.01	42
50 ppm THPS + 100 nM Peptide A	1.5 ± 0.5	0.10 ± 0.03	60
100 ppm THPS	0.3 ± 0.2	0.02 ± 0.01	92

seed culture. Each glass cell consisted of a 13Cr WE (working electrode) (1 cm × 1 cm) and a graphite rod (0.64 cm diameter and 1 cm height) counter electrode, which also served as reference electrode. Electrochemical scans were performed using a PCI4/750 potentiostat (Gamry Instruments, Inc., Warminster, PA, United States). Linear polarization resistance (LPR) and Tafel were scanned daily during the 7-day incubation period. LPR measurement was performed within the range of −10 to 10 mV vs. OCP (open circuit potential) with a rate of 0.167 mV/s. Tafel curves were scanned at a scan rate of 0.167 mV/s from OCP to −200 mV vs. OCP, and then after a 20 min gap, from OCP to +200 mV vs. OCP on the same working electrode (Wang et al., 2021a; Xu et al., 2023b). It was shown that this dual half-scan scheme with the voltage range did not alter the working electrode in repeated scans on the same working electrode (Wang et al., 2022a).

3 Results and discussion

3.1 Sessile cell count

Figure 1 shows images of 125 mL anaerobic vials before and after the 7-day incubation. *D. ferrophilus* growth was seen in vials with no treatment, 50 ppm THPS and 50 ppm THPS + 100 nM Peptide A. With 100 ppm THPS, no apparent planktonic growth was observed (not turbid), suggesting strong inhibition effect. Table 4 summarizes sessile cell counts on coupons with different treatment.

Without biocide treatment, sessile cells on 13Cr coupons were found to be (3.9 ± 0.8) × 10^7 cells/cm^2. With treatment of 50 ppm THPS and 50 ppm THPS + 100 nM Peptide A, sessile cell counts reduced to (8.0 ± 0.4) × 10^6 cells/cm^2 and

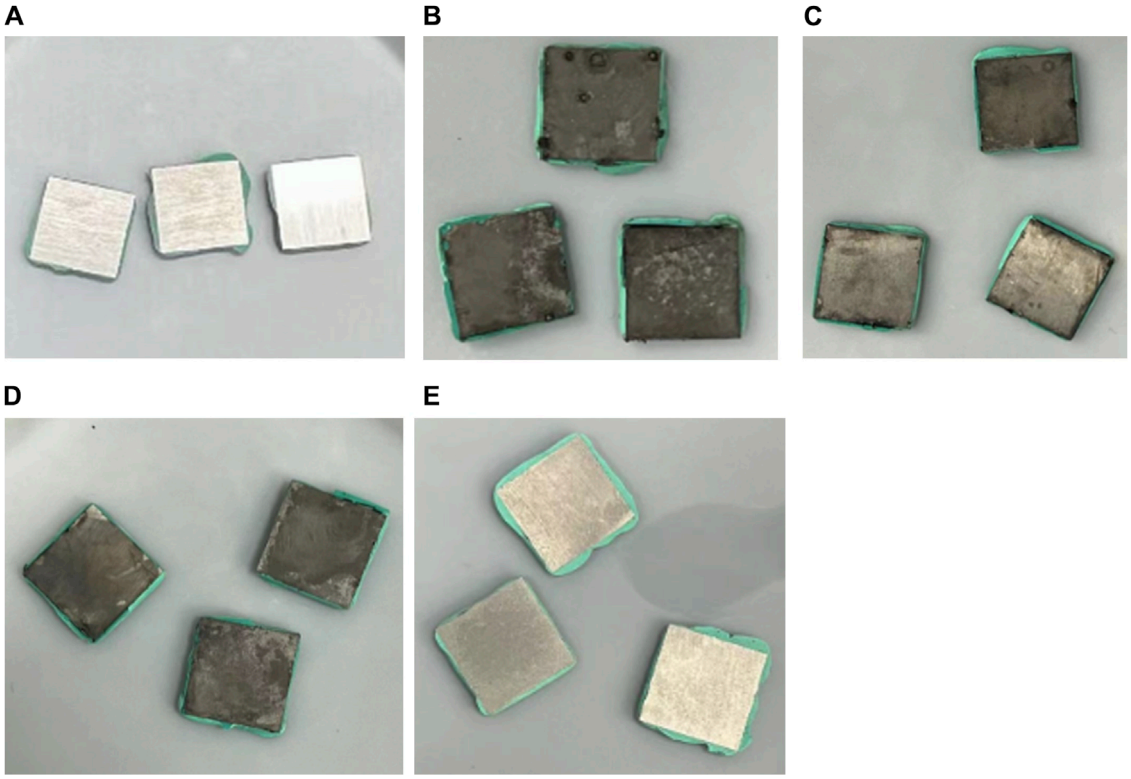

FIGURE 3
13Cr coupons after Clarke's solution cleaning treatment following 7-day *D. ferrophilus* incubation in EASW: **(A)** abiotic control, **(B)** no treatment, **(C)** 50 ppm THPS, **(D)** 50 ppm THPS + 100 nM Peptide A, and **(E)** 100 ppm THPS.

(2.4 ± 0.4) × 10^6 cells/cm^2. A 0.7-log reduction was seen in sessile cells with 50 ppm THPS alone, and the addition of 100 nM Peptide A achieved an extra 0.5-log reduction, showing its obvious enhancement effect. Sessile cells were not detected (detection threshold of 5 × 10^4 planktonic cells/mL translating into 5 × 10^4 sessile cells/cm^2) on coupons treated with 100 ppm THPS.

3.2 Biofilm CLSM images

CLSM images of *D. ferrophilus* biofilms on 13Cr coupon surfaces with different treatments are presented in Figure 2. Healthy biofilms were seen on the coupon surface without treatment (Figure 2A) with densely populated green dots (live cells). With 50 ppm THPS and 50 ppm THPS + 100 nM Peptide A (Figures 2B, C), live cells became fewer and more dead cells (red dots) appeared. It is hard to see any live cells in Figure 2D on the 13Cr coupon surface treated with 100 ppm THPS. Here, these CLSM biofilm observations are consistent with the sessile cell count results.

3.3 Weight loss

The weight loss results of 13Cr coupons with different treatment are listed in Table 5. For the abiotic control, no weight loss was detected. The weight losses for coupons with no treatment, 50 ppm THPS, 50 ppm THPS + 100 nM Peptide A and 100 ppm THPS were 3.8 ± 0.5 mg/cm^2 (equivalent to uniform corrosion rate 0.26 ± 0.03 mm/a), 2.2 ± 0.2 mg/cm^2 (0.15 ± 0.01 mm/a), 1.5 ± 0.5 mg/cm^2 (0.10 ± 0.03 mm/a) and 0.3 ± 0.2 mg/cm^2 (0.02 ± 0.01 mm/a), respectively. THPS at 50 ppm reduced weight loss by 42%, while 50 ppm THPS + 100 nM Peptide A achieved an extra 18% weight loss reduction, suggesting considerable enhancement effect. With 100 ppm THPS, the uniform corrosion inhibition efficiency reached 92% which was very effective. In EET-MIC by SRB, sessile cells in biofilms are directly involved in iron oxidation. The weight loss sequence matches the sessile cell count sequence. Thus, the greatly reduced weight loss here can be attributed to the effectiveness of THPS in inhibiting the growth of *D. ferrophilus* biofilms and the biofilm dispersing effect of Peptide A.

The outstanding performance of THPS in mitigating SRB MIC was because the degradation of THPS forms trihydroxymethyl phosphine which can destroy microbial cell walls by reducing disulfide bonds within cell wall disulfide amino acids (Parker and Kharasch, 1959; Rüegg and Rudinger, 1977). THPS also inhibits SRB growth through its selective action which affects the hNRB (heterotrophic nitrate-reducing bacteria) and so-NRB (sulfide-oxidizing-NRB) activities (Okoro, 2015). Besides, as an H_2S scavenger, THPS can mitigate corrosion caused by souring (Talbot et al., 2000). The biofilm dispersing effect of Peptide A enhanced the THPS treatment effect as some sessile cells

10.3389/fmats.2024.1407655

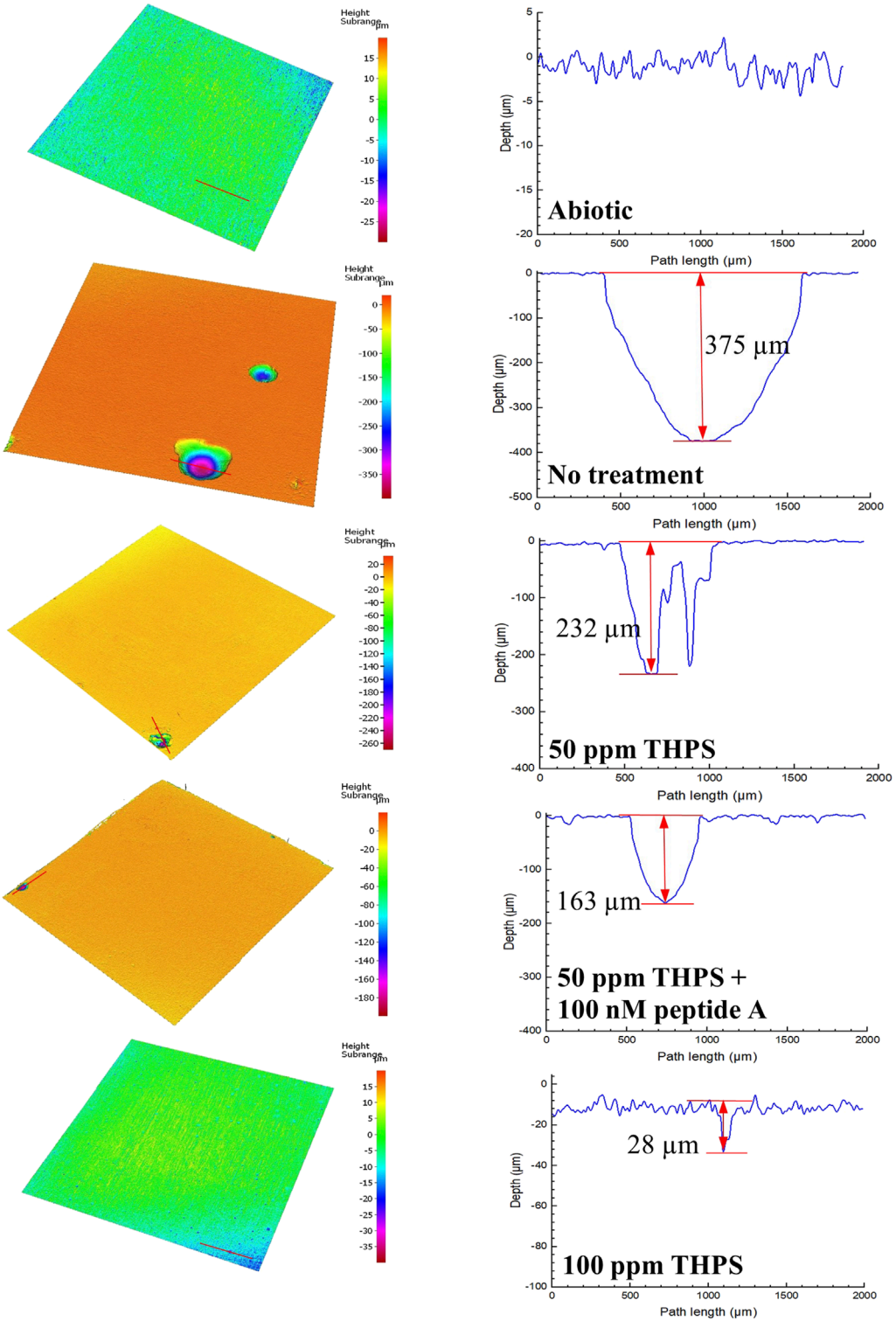

FIGURE 4
Pit images and profiles from IFM for 13Cr coupons after 7-day *D. ferrophilus* incubation in EASW in anaerobic vials. (Red lines indicate IFM pit profile scan paths.)

were detached without biocide kill. The exact mechanism for Peptide A's superior biofilm dispersing ability remains unknown, but it likely functions as a signal molecule. Thus, its effective dosage is extremely small, much lower than the 10s of ppm dosage required for a typical corrosion inhibitor that needs to have a monolayer coverage on a metal surface.

TABLE 6 Calculated *RPS* values for different treatment.

	No treatment	50 ppm THPS	50 ppm THPS + 100 nM peptide A	100 ppm THPS
Uniform corrosion rate (mm/a)	0.26	0.15	0.10	0.02
Pitting rate (mm/a)	20	12	8.6	1.5
RPS	77	80	86	75

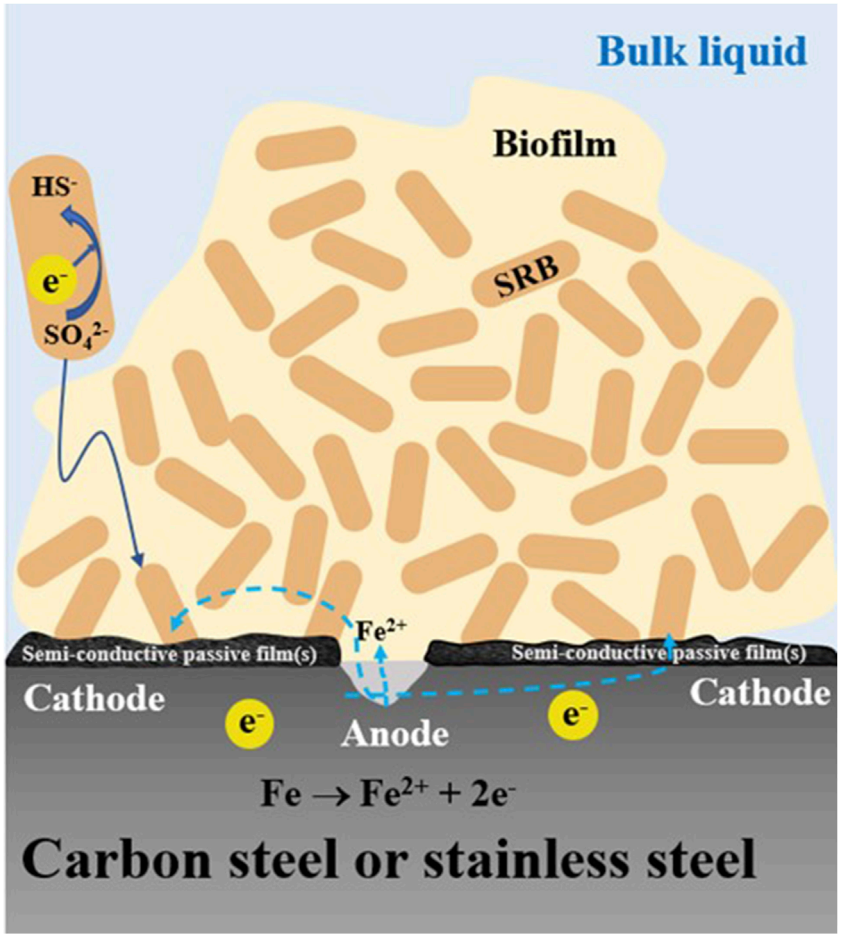

FIGURE 5
Schematic illustration showing small anode-large cathode with semi-conductive passive film(s) scenario leading to severe pitting with an isolated large pit.

3.4 Pitting analysis

Coupons with biofilms and corrosion products removed are shown in Figures 3A–E. Some corrosion pits on the coupons are visible to the naked eyes, especially for coupons without treatment in Figure 3B. Figure 4 presents pits with maximum depth and pit profiles scanned using IFM. No well-defined pits were found on the abiotic coupon surface. The maximum pit depth for coupons with no treatment, 50 ppm THPS, 50 ppm THPS + 100 nM Peptide A and 100 ppm THPS were 375 μm (equivalent to 20 mm/a pitting rate), 232 μm (12 mm/a), 163 μm (8.6 mm/a) and 28 μm (1.5 mm/a), respectively. The single deepest pit on the coupon without treatment alone results in a weigh loss of 1.95 mg, accounting for 42% of the entire coupon weight loss. The addition of 50 ppm THPS, 50 ppm THPS + 100 nM Peptide A and 100 ppm THPS reduced pitting rates by 38%, 57%, and 93%, respectively. Thus, 100 ppm THPS mitigated pitting corrosion greatly.

Based on the uniform corrosion rates from weight loss data and pitting corrosion rates, *RPS* were calculated and summarized in Table 6. The *RPS* for 13Cr in all conditions were all considerably

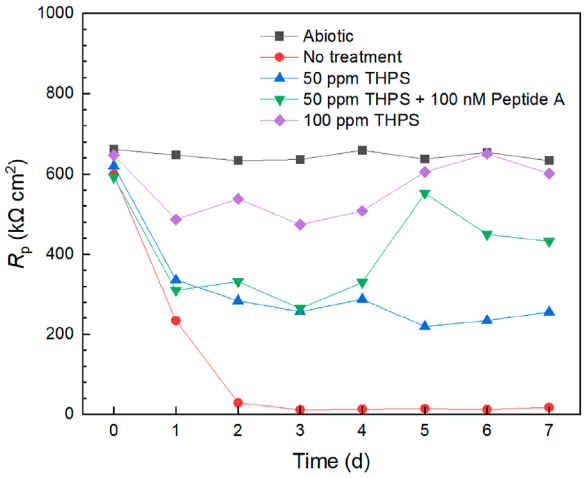

FIGURE 6
R_p curves from LPR measurements during 7-day *D. ferrophilus* incubation in 10 mL electrochemical glass cell.

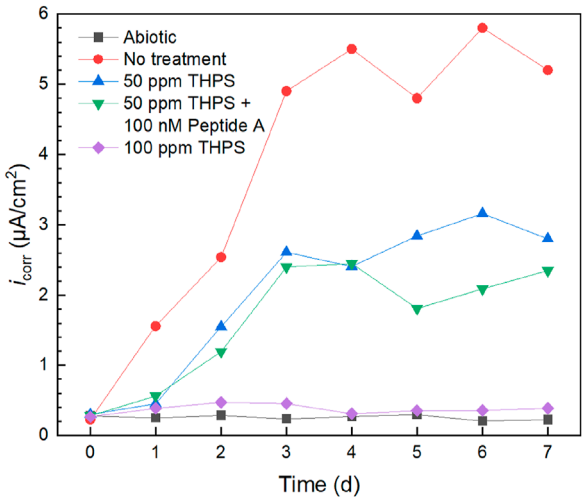

FIGURE 7
i_{corr} vs. time during 7-day *D. ferrophilus* incubation in 10 mL electrochemical glass cell.

high but similar with an average value of 80. In comparison, *RPS* of C1018 carbon steel MIC by *D. ferrophilus* in EASW was only 1.36 (Wang et al., 2021a). This phenomenon supported the fact that pitting corrosion is the major issue for low grade stainless steels just like 13Cr. Even with biocide treatment, the *RPS* values showed no apparent changes, which were still almost two orders of magnitude of that for C1018 carbon steel. With 100 ppm THPS, the uniform corrosion rate declined to a very small number of 0.02 mm/a. However, its pitting rate was still as high as 1.5 mm/a, which is greater than pitting rates of some carbon steels in the same system without any biocide treatment (Wang et al., 2021a; Xu et al., 2023b). Thus, a higher THPS dosage may be needed for better biocide mitigation to prevent pinhole leaks due to SRB MIC pitting.

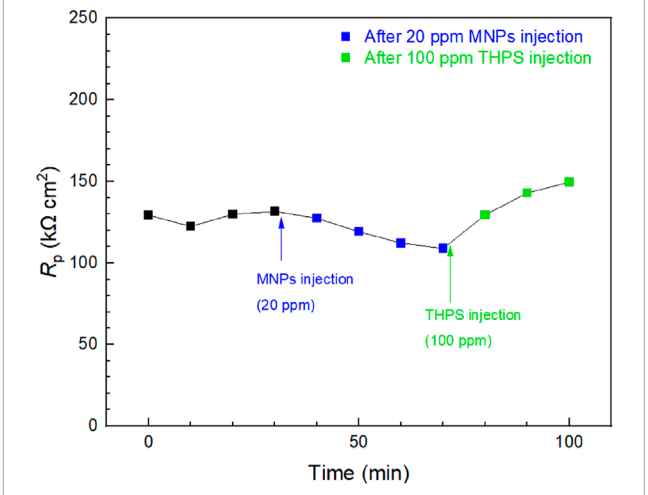

FIGURE 8
R_p responses of 13Cr to tandem injections of MNPs and THPS in 10 mL electrochemical glass cell containing 3-day old *D. ferrophilus*. (Time zero indicates injection at 3 days of incubation.)

The high *PRS* values in Table 6 for 13Cr shows that it is particularly prone to pitting corrosion. 13Cr is a low-grade stainless steel (420 SS) with a PREN (pitting resistance equivalent number) value of 13. It has a passive film that is relatively easy to be damaged in some spots compared to higher grade stainless steels such as 304 SS with a PREN value of 20 (L. Xu et al., 2023b). CrSs have Cr oxide/hydroxide passive films that are (semi-)conductive (Sun et al., 2016). In SRB MIC, the iron sulfide corrosion product film is also (semi-)conductive (Gu et al., 2019). Thus, 13Cr MIC by SRB satisfies the two essential requirements for classical pitting, i.e., a passive film that can be damaged and the passive film is (semi-)conductive (L. Xu et al., 2023b). This leads to a large cathode to small anode area ratio situation, which amplifies the pitting effect as illustrated in Figure 5. In carbon steel MIC by SRB, the corrosion products (iron sulfides) form a conductive film that can reach 10–30 μm in thickness (Jia et al., 2018). In stainless steel MIC by SRB, the iron sulfides film will be on top of the metal's own passive film (chromium oxides/chromium hydroxide) that is only several nm in thickness (Mohammadi et al., 2011). Sessile cells in the biofilm can harvest electrons across both (semi-)conductive films.

3.5 Electrochemical measurements

Electrochemical tests can provide extra evidence, especially transient information, to support one-shoot weight loss data. Figure 6 demonstrates R_p (polarization resistance) variations of 13Cr with different treatment from LPR measurements. The abiotic control exhibited a stable curve over the 7-day incubation. Without treatment, R_p declined considerably from 1 day to 3 days and remained stable for the remaining time. This suggests that mature biofilm formed at 3 days and corrosion rate generally increased during the first 3 days and stabilized from 3 days to 7 days. With 50 ppm THPS, the R_p curve was consistently higher

than that of no treatment. Compared with 50 ppm THPS alone, R_p values of 50 ppm THPS + 100 nM Peptide A were generally higher, especially from 5 days to 7 days. Thus, the enhancement effect of Peptide A for THPS was clearly manifested. The R_p values of 100 ppm THPS did not drop considerably compared to the abiotic control and remained high during the 7-d incubation period, indicating effective corrosion inhibition through biofilm inhibition. The $1/R_p$ sequence of different treatments matches the corrosion rate sequence based on weight loss results. Based on the $1/R_p$ data at 7 days, 100 ppm THPS achieved a corrosion inhibition efficiency of 97%.

Corrosion current density (i_{corr}) results fitted from 7-day Tafel scans are displayed in Figure 7. Without treatment, i_{corr} gradually increased and remained higher than the treated conditions. With 100 nM Peptide A, i_{corr} values of 100 ppm THPS were generally lower than those without over the entire 7-day incubation period. The 100 ppm THPS i_{corr} kept at a low level which was close to the abiotic control, proving that 100 ppm THPS was effective in biofilm inhibition. The i_{corr} sequence of different treatments again matches the weight loss sequence. Based on the i_{corr} data at 7 days, 100 ppm THPS achieved a corrosion inhibition efficiency of 93%. It should be noted that daily Tafel scans of the same WE were permitted using the dual-scan method with cathodic scan and cathodic scan commencing at OCP according to our previous Tafel scan scheme study (Wang et al., 2022a). Both LPR and Tafel findings confirmed the effective mitigation of *D. ferrophilus* MIC on 13Cr and the obvious enhancement effect of Peptide A for THPS. They provide extra evidence to support weight loss or uniform corrosion results. The overall corrosion rates were substantially reduced with biocide addition which also resulted in much lower pitting rates as reflected by the pitting analysis.

Injection tests were conducted in a 10 mL electrochemical cell at 3 days when mature *D. ferrophilus* biofilms formed on the 13Cr WE surface. In Figure 8, stable R_p readings were obtained for 40 min before injections. After 20 ppm (final concentration in the broth) MNPs injection, a generally decreasing R_p trend was observed and R_p was reduced by 16% in 40 min after the injection, which means the corrosion rate became higher. This shows that MNPs successfully enhanced MIC of *D. ferrophilus* against 13Cr. THPS was subsequently injected to reach 100 ppm in broth and led to an increase in R_p. The final R_p value was increased by 37% due to the THPS injection, indicating mitigation effect of THPS.

The 16% R_p decreased after the injection of MNPs was because MIC of 13Cr by *D. ferrophilus* belongs to EET-MIC where the electron transfer between sessile cell walls and Fe surface is an important rate-limiting process, and the MNPs can serve as electron conduits to accelerate this process (Wang et al., 2022b). Thus, the SRB MIC of 13Cr is proven to be EET-MIC here. The followed THPS injection proved its biocidal effect in treating SRB biofilms and showed that electrochemical injection tests were sensitive enough to provide both accelerated and decelerated MIC information. It should be noted that treating a pre-established biofilm is far more difficult than preventing the biofilm from establishing. Thus, 37% was much smaller than the 93% based on the i_{corr} data at 7 days in Figure 7.

4 Conclusion

Severe pitting corrosion was found on 13Cr after the 7-day incubation. THPS was effective in mitigating *D. ferrophilus* MIC against 13Cr. The enhancement effect of Peptide A for THPS was manifested. The macroscopic pits on 13Cr coupon surfaces visible to the naked eyes disappeared with effective biocide treatment. However, to reduce pitting corrosion completely, a THPS dosage higher than 100 ppm will be needed.

The electrochemical results in this work indicate that electrochemical measurements qualitatively described biocide treatment efficacy consistent with sessile cell count and weight loss data trends.

This lab investigation demonstrated an alarming SRB pitting risk for 13Cr. If 13Cr is used to combat CO_2 (uniform) corrosion in the presence of SRB, a biocide mitigation plan should be in place to prevent pinhole leaks caused by potentially very fast SRB pitting.

Data availability statement

The raw data supporting the conclusion of this article will be made available by the authors, without undue reservation.

Author contributions

LX: Data curation, Formal Analysis, Investigation, Methodology, Validation, Visualization, Writing–original draft. AK: Data curation, Investigation, Methodology, Writing–original draft. PK: Conceptualization, Resources, Writing–review and editing. SK: Conceptualization, Resources, Writing–review and editing. SP: Conceptualization, Resources, Writing–review and editing. TG: Funding acquisition, Methodology, Project administration, Supervision, Validation, Writing–review and editing.

Funding

The author(s) declare that financial support was received for the research, authorship, and/or publication of this article. This work was financially supported by PTT Exploration and Production, and Petrobras.

Acknowledgments

We thank Flavia Maciel Fernandes Guedes, Vinicius de Abreu Waldow, Maira Paula de Sousa, Rubens Nobumoto Akamine, and Gustavo Leitao Vaz for their expertise and input throughout this study.

Conflict of interest

Authors PK, SK, and SP were employed by PTT Exploration and Production.

The remaining authors declare that the research was conducted in the absence of any commercial or financial relationships that could be construed as a potential conflict of interest.

The author(s) declared that they were an editorial board member of Frontiers, at the time of submission. This had no impact on the peer review process and the final decision.

Publisher's note

All claims expressed in this article are solely those of the authors and do not necessarily represent those of their affiliated organizations, or those of the publisher, the editors and the reviewers. Any product that may be evaluated in this article, or claim that may be made by its manufacturer, is not guaranteed or endorsed by the publisher.

References

Abbas, M. A., Zakaria, K., El-Shamy, A. M., and Abedin, S. Z. E. (2021). Utilization of 1-butylpyrrolidinium chloride ionic liquid as an eco-friendly corrosion inhibitor and biocide for oilfield equipment: combined weight loss, electrochemical and SEM studies. *Z. Für Phys. Chem.* 235, 377–406. doi:10.1515/zpch-2019-1517

Abdalla Filho, J., Machado, R., Bertin, R., and Valentini, M. (2014). On the failure pressure of pipelines containing wall reduction and isolated pit corrosion defects. *Comput. Struct.* 132, 22–33. doi:10.1016/j.compstruc.2013.10.017

Abdullah, A., Yahaya, N., Md Noor, N., and Mohd Rasol, R. (2014). Microbial corrosion of API 5L X-70 carbon steel by ATCC 7757 and consortium of sulfate-reducing bacteria. *J. Chem.* 2014, 1–7. doi:10.1155/2014/130345

Alcántara, J., de la Fuente, D., Chico, B., Simancas, J., Díaz, I., and Morcillo, M. (2017). Marine atmospheric corrosion of carbon steel: a review. *Materials* 10, 406. doi:10.3390/ma10040406

Astuti, D., Purwasena, I. A., and Putri, F. Z. (2018). Potential of biosurfactant as an alternative biocide to control biofilm associated biocorrosion. *J. Environ. Sci. Technol.* 11, 104–111. doi:10.3923/jest.2018.104.111

Bhandari, J., Khan, F., Abbassi, R., Garaniya, V., and Ojeda, R. (2015). Modelling of pitting corrosion in marine and offshore steel structures–A technical review. *J. Loss Prev. Process Ind.* 37, 39–62. doi:10.1016/j.jlp.2015.06.008

Blais, J.-F., Djedidi, Z., Cheikh, R. B., Tyagi, R. D., and Mercier, G. (2008). Metals precipitation from effluents: review. *Toxic. Radioact. Waste Manag.* 12, 135–149. doi:10.1061/(asce)1090-025x(2008)12:3(135)

Černoušek, T., Shrestha, R., Kovářová, H., Špánek, R., Ševců, A., Sihelská, K., et al. (2020). Microbially influenced corrosion of carbon steel in the presence of anaerobic sulphate-reducing bacteria. *Corros. Eng. Sci. Technol.* 55, 127–137. doi:10.1080/1478422X.2019.1700642

Chouchaoui, B., and Pick, R. (1996). Behaviour of longitudinally aligned corrosion pits. *Int. J. Press. Vessels Pip.* 67, 17–35. doi:10.1016/0308-0161(94)00057-3

Chugh, B., Thakur, S., and Singh, A. K. (2020). Microbiologically influenced corrosion inhibition in oil and gas industry. *Corros. Inhib. Oil Gas. Ind.*, 321–338. doi:10.1002/9783527822140.ch13

Conlette, O. (2014). Impacts of tetrakis-hydroxymethyl phosphonium sulfate (THPS) based biocides on the functional group activities of some oil field microorganisms associated with corrosion and souring. *Br. Microbiol. Res. J.* 4, 1463–1475. doi:10.9734/BMRJ/2014/11943

Costa, E. M., Dedavid, B. A., Santos, C. A., Lopes, N. F., Fraccaro, C., Pagartanidis, T., et al. (2023). Crevice corrosion on stainless steels in oil and gas industry: a review of techniques for evaluation, critical environmental factors and dissolved oxygen. *Eng. Fail. Anal.* 144, 106955. doi:10.1016/j.engfailanal.2022.106955

Dong, Y., Lekbach, Y., Li, Z., Xu, D., El Abed, S., Ibnsouda Koraichi, S., et al. (2020). Microbiologically influenced corrosion of 304L stainless steel caused by an alga associated bacterium *Halomonas titanicae*. *J. Mater. Sci. Technol.* 37, 200–206. doi:10.1016/j.jmst.2019.06.023

Dorcheh, A. S., Durham, R. N., and Galetz, M. C. (2016). Corrosion behavior of stainless and low-chromium steels and IN625 in molten nitrate salts at 600 °C. *Sol. Energy Mater. Sol. Cells* 144, 109–116. doi:10.1016/j.solmat.2015.08.011

Dou, W., Jia, R., Jin, P., Liu, J., Chen, S., and Gu, T. (2018). Investigation of the mechanism and characteristics of copper corrosion by sulfate reducing bacteria. *Corros. Sci.* 144, 237–248. doi:10.1016/j.corsci.2018.08.055

Dwivedi, D., Lepková, K., and Becker, T. (2017). Carbon steel corrosion: a review of key surface properties and characterization methods. *RSC Adv.* 7, 4580–4610. doi:10.1039/c6ra25094g

El-Shamy, A. M. (2020). A review on: biocidal activity of some chemical structures and their role in mitigation of microbial corrosion. Egypt. *J. Chem.* 63, 5251–5267. doi:10.21608/ejchem.2020.32160.2683

Enning, D., and Garrelfs, J. (2014). Corrosion of iron by sulfate-reducing bacteria: new views of an old problem. *Appl. Environ. Microbiol.* 80, 1226–1236. doi:10.1128/aem.02848-13

Enning, D., Venzlaff, H., Garrelfs, J., Dinh, H. T., Meyer, V., Mayrhofer, K., et al. (2012). Marine sulfate-reducing bacteria cause serious corrosion of iron under electroconductive biogenic mineral crust. *Environ. Microbiol.* 14, 1772–1787. doi:10.1111/j.1462-2920.2012.02778.x

Ettefagh, A. H., Guo, S., and Raush, J. (2021). Corrosion performance of additively manufactured stainless steel parts: a review. *Addit. Manuf.* 37, 101689. doi:10.1016/j.addma.2020.101689

Fahim, A., Dean, A. E., Thomas, M. D., and Moffatt, E. G. (2019). Corrosion resistance of chromium-steel and stainless steel reinforcement in concrete. *Mater. Corros.* 70, 328–344. doi:10.1002/maco.201709942

Gana, M. L., Kebbouche-Gana, S., Touzi, A., Zorgani, M. A., Pauss, A., Lounici, H., et al. (2011). Antagonistic activity of Bacillus sp. obtained from an Algerian oilfield and chemical biocide THPS against sulfate-reducing bacteria consortium inducing corrosion in the oil industry. *J. Ind. Microbiol. Biotechnol.* 38, 391–404. doi:10.1007/s10295-010-0887-2

Grande Burgos, M. J., Lucas López, R., López Aguayo, M. del C., Pérez Pulido, R., and Gálvez, A. (2013). Inhibition of planktonic and sessile *Salmonella enterica* cells by combinations of enterocin AS-48, polymyxin B and biocides. *Food control.* 30, 214–221. doi:10.1016/j.foodcont.2012.07.011

Gu, T., Jia, R., Unsal, T., and Xu, D. (2019). Toward a better understanding of microbiologically influenced corrosion caused by sulfate reducing bacteria. *J. Mater. Sci. Technol.* 35, 631–636. doi:10.1016/j.jmst.2018.10.026

Hinds, G., Zhao, J., and Turnbull, A. (2005). Hydrogen diffusion in super 13% chromium martensitic stainless steel. *Corrosion* 61, 348–354. doi:10.5006/1.3279887

Jia, R., Tan, J. L., Jin, P., Blackwood, D. J., Xu, D., and Gu, T. (2018). Effects of biogenic H2S on the microbiologically influenced corrosion of C1018 carbon steel by sulfate reducing *Desulfovibrio vulgaris* biofilm. *Corros. Sci.* 130, 1–11. doi:10.1016/j.corsci.2017.10.023

Jia, R., Yang, D., Dou, W., Liu, J., Zlotkin, A., Kumseranee, S., et al. (2019). A sea anemone-inspired small synthetic peptide at sub-ppm concentrations enhanced biofilm mitigation. *Int. Biodeterior. Biodegr.* 139, 78–85. doi:10.1016/j.ibiod.2018.11.009

Kermani, M. B., and Harrop, D. (1996). The impact of corrosion on the oil and gas industry. *SPE Prod. Facil.* 11, 186–190. doi:10.2118/29784-PA

Lin, X., Liu, W., Wu, F., Xu, C., Dou, J., and Lu, M. (2015). Effect of O2 on corrosion of 3Cr steel in high temperature and high pressure CO2–O2 environment. *Appl. Surf. Sci.* 329, 104–115. doi:10.1016/j.apsusc.2014.12.109

Mesquita, T. J., Chauveau, E., Mantel, M., Bouvier, N., and Koschel, D. (2014). Corrosion and metallurgical investigation of two supermartensitic stainless steels for oil and gas environments. *Corros. Sci.* 81, 152–161. doi:10.1016/j.corsci.2013.12.015

Mohammadi, F., Nickchi, T., Attar, M., and Alfantazi, A. (2011). EIS study of potentiostatically formed passive film on 304 stainless steel. *Electrochimica Acta* 56, 8727–8733. doi:10.1016/j.electacta.2011.07.072

Mukherjee, A., and Ahn, Y.-H. (2022). Terpinolene as an enhancer for ultrasonic disinfection of multi-drug-resistant bacteria in hospital wastewater. *Environ. Sci. Pollut. Res.* 29, 34500–34514. doi:10.1007/s11356-022-18611-6

Obot, I., Onyeachu, I. B., Umoren, S. A., Quraishi, M. A., Sorour, A. A., Chen, T., et al. (2020). High temperature sweet corrosion and inhibition in the oil and gas industry: progress, challenges and future perspectives. *J. Pet. Sci. Eng.* 185, 106469. doi:10.1016/j.petrol.2019.106469

Okoro, C. (2015). The biocidal efficacy of tetrakis-hydroxymethyl phosphonium sulfate (THPS) based biocides on oil pipeline pigruns liquid biofilms. *Pet. Sci. Technol.* 33, 1366–1372. doi:10.1080/10916466.2015.1062781

Parker, A. J., and Kharasch, N. (1959). The scission of the sulfur-sulfur bond. *Chem. Rev.* 59, 583–628. doi:10.1021/cr50028a003

Pu, Y., Tian, Y., Hou, S., Dou, W., and Chen, S. (2023). Enhancement of exogenous riboflavin on microbiologically influenced corrosion of nickel by electroactive *Desulfovibrio vulgaris* biofilm. *npj Mater. Degrad.* 7, 7. doi:10.1038/s41529-023-00325-w

Rüegg, U. T., and Rudinger, J. (1977). "Reductive cleavage of cystine disulfides with tributylphosphine," in *Methods in enzymology*, 111–116.

Sand, W., and Gehrke, T. (2003). Microbially influenced corrosion of steel in aqueous environments. *Rev. Environ. Sci. Biotechnol.* 2, 169–176. doi:10.1023/B:RESB.0000040468.88570.4e

Scheuer, C., Possoli, F., Borges, P., Cardoso, R., and Brunatto, S. (2019). AISI 420 martensitic stainless steel corrosion resistance enhancement by low-temperature plasma carburizing. *Electrochimica Acta* 317, 70–82. doi:10.1016/j.electacta.2019.05.101

Sheng, X., Ting, Y.-P., and Pehkonen, S. O. (2007). The influence of sulphate-reducing bacteria biofilm on the corrosion of stainless steel AISI 316. *Corros. Sci.* 49, 2159–2176. doi:10.1016/j.corsci.2006.10.040

Shi, X., Zhang, R., Sand, W., Mathivanan, K., Zhang, Y., Wang, N., et al. (2023). Comprehensive review on the use of biocides in microbiologically influenced corrosion. *Microorganisms* 11, 2194. doi:10.3390/microorganisms11092194

Silva, P., Oliveira, S. H., Vinhas, G. M., Carvalho, L. J., Barauna, O. S., Urtiga Filho, S. L., et al. (2021). Tetrakis hydroxymethyl phosphonium sulfate (THPS) with biopolymer as strategy for the control of microbiologically influenced corrosion in a dynamic system. *Chem. Eng. Process.-Process Intensif.* 160, 108272. doi:10.1016/j.cep.2020.108272

Skovhus, T. L., Eckert, R. B., and Rodrigues, E. (2017). Management and control of microbiologically influenced corrosion (MIC) in the oil and gas industry—overview and a North Sea case study. *J. Biotechnol.* 256, 31–45. doi:10.1016/j.jbiotec.2017.07.003

Sun, J., Sun, C., and Wang, Y. (2016). Effect of Cr content on the electrochemical behavior of low-chromium X65 steel in CO_2 environment. *Int. J. Electrochem Sci.* 11, 8599–8611. doi:10.20964/2016.10.58

Talbot, R. E., Larsen, J., and Sanders, P. F. (2000). Experience with the use of tetrakishydroxymethylphosphonium sulfate (THPS) for the control of downhole hydrogen sulfide. Paper Number: NACE-00123, presented at CORROSION 2000 Conference, Orlando, Florida, March, 2000.

Thauer, R. K., Stackebrandt, E., and Hamilton, W. A. (2007). Energy metabolism and phylogenetic diversity of sulphate-reducing bacteria. In: *Sulphate-Reducing Bact.* Editors L. L. Barton, and W. A. Hamilton, 1–38. doi:10.1017/cbo9780511541490.002

Unsal, T., Wang, D., Kumseranee, S., Punpruk, S., Mohamed, M.E.-S., Saleh, M. A., et al. (2021). Assessment of 2,2-dibromo-3-nitrilopropionamide biocide enhanced by D-tyrosine against zinc corrosion by a sulfate reducing bacterium. *Ind. Eng. Chem. Res.* 60, 4009–4018. doi:10.1021/acs.iecr.0c06317

Videla, H. A., and Characklis, W. G. (1992). Biofouling and microbially influenced corrosion. *Int. Biodeterior. Biodegr. Spec. Issue Microbially Influ. Corros.* 29, 195–212. doi:10.1016/0964-8305(92)90044-O

Wang, B., Xu, L., Zhu, J., Xiao, H., and Lu, M. (2016). Observation and analysis of pseudopassive film on 6.5%Cr steel in CO_2 corrosion environment. *Corros. Sci.* 111, 711–719. doi:10.1016/j.corsci.2016.06.006

Wang, D., Kijkla, P., Mohamed, M. E., Saleh, M. A., Kumseranee, S., Punpruk, S., et al. (2021a). Aggressive corrosion of carbon steel by *Desulfovibrio ferrophilus* IS5 biofilm was further accelerated by riboflavin. *Bioelectrochemistry* 142, 107920. doi:10.1016/j.bioelechem.2021.107920

Wang, D., Kijkla, P., Saleh, M. A., Kumseranee, S., Punpruk, S., and Gu, T. (2022a). Tafel scan schemes for microbiologically influenced corrosion of carbon steel and stainless steel. *J. Mater. Sci. Technol.* 130, 193–197. doi:10.1016/j.jmst.2022.05.018

Wang, D., Liu, J., Jia, R., Dou, W., Kumseranee, S., Punpruk, S., et al. (2020). Distinguishing two different microbiologically influenced corrosion (MIC) mechanisms using an electron mediator and hydrogen evolution detection. *Corros. Sci.* 177, 108993. doi:10.1016/j.corsci.2020.108993

Wang, D., Yang, C., Saleh, M. A., Alotaibi, M. D., Mohamed, M. E., Xu, D., et al. (2022b). Conductive magnetite nanoparticles considerably accelerated carbon steel corrosion by electroactive *Desulfovibrio vulgaris* biofilm. *Corros. Sci.* 205, 110440. doi:10.1016/j.corsci.2022.110440

Wu, Q., Zhang, Z., Dong, X., and Yang, J. (2013). Corrosion behavior of low-alloy steel containing 1% chromium in CO_2 environments. *Corros. Sci.* 75, 400–408. doi:10.1016/j.corsci.2013.06.024

Xu, D., and Gu, T. (2014). Carbon source starvation triggered more aggressive corrosion against carbon steel by the *Desulfovibrio vulgaris* biofilm. *Int. Biodeterior. Biodegr.* 91, 74–81. doi:10.1016/j.ibiod.2014.03.014

Xu, D., Gu, T., and Lovley, D. R. (2023). Microbially mediated metal corrosion. *Nat. Rev. Microbiol.* 21, 705–718. doi:10.1038/s41579-023-00920-3

Xu, L., Ivanova, S. A., and Gu, T. (2023a). Mitigation of galvanized steel biocorrosion by *Pseudomonas aeruginosa biofilm* using a biocide enhanced by trehalase. *Bioelectrochemistry* 154, 108508. doi:10.1016/j.bioelechem.2023.108508

Xu, L., Kijkla, P., Kumseranee, S., Punpruk, S., and Gu, T. (2023b). "Corrosion-resistant" chromium steels for oil and gas pipelines can suffer from very severe pitting corrosion by a sulfate-reducing bacterium. *J. Mater. Sci. Technol. S1005030223001287* 174, 23–29. doi:10.1016/j.jmst.2023.01.008

Yang, X., Shao, J., Liu, Z., Zhang, D., Cui, L., Du, C., et al. (2020). Stress-assisted microbiologically influenced corrosion mechanism of 2205 duplex stainless steel caused by sulfate-reducing bacteria. *Corros. Sci.* 173, 108746. doi:10.1016/j.corsci.2020.108746

Yazdi, M., Khan, F., and Abbassi, R. (2021). Microbiologically influenced corrosion (MIC) management using Bayesian inference. *Ocean. Eng.* 226, 108852. doi:10.1016/j.oceaneng.2021.108852

You, X., Xu, N., Yang, X., and Sun, W. (2021). Pollutants affect algae-bacteria interactions: a critical review. *Environ. Pollut.* 276, 116723. doi:10.1016/j.envpol.2021.116723